Published in final edited form as:
Arch Insect Biochem Physiol. 2013 February ; 82(2): 96–115. doi:10.1002/arch.21078.

Functional Analysis of a Mosquito Short Chain Dehydrogenase Cluster

Jaime G. Mayoral[¶,#], **Kate T. Leonard**[¶], **Lucas A. Defelipe**[†], **Adrian G. Turjansksi**[†], **Marcela Nouzova**[¶], and **Fernando G. Noriegal**[¶]

[¶]Dept. Biological Sciences. Florida International University, Miami, FL, 33199, USA

[†]Departamento de Química Biológica, Facultad de Ciencias Exactas y Naturales, Universidad de Buenos Aires e INQUIMAE/CONICET, Buenos Aires, Argentina

Abstract

The short chain dehydrogenases (SDR) constitute one the oldest and largest families of enzymes with over 46,000 members in sequence databases. About 25% of all known dehydrogenases belong to the SDR family. SDR enzymes have critical roles in lipid, amino acid, carbohydrate, hormone and xenobiotic metabolism as well as in redox sensor mechanisms. This family is present in archaea, bacteria, and eukaryota, emphasizing their versatility and fundamental importance for metabolic processes. We identified a cluster of eight SDRs in the mosquito *Aedes aegypti* (AaSDRs). Members of the cluster differ in tissue specificity and developmental expression. Heterologous expression produced recombinant proteins that had diverse substrate specificities, but distinct from the conventional insect alcohol (ethanol) dehydrogenases. They are all NADP+-dependent and they have S-enantioselectivity and preference for secondary alcohols with 8–15 carbons. Homology modeling was used to build the structure of AaSDR1 and two additional cluster members. The computational study helped explain the selectivity towards the (10S)-isomers as well as the reduced activity of AaSDR4 and AaSDR9 for longer isoprenoid substrates. Similar clusters of SDRs are present in other species of insects, suggesting similar selection mechanisms causing duplication and diversification of this family of enzymes.

Keywords

alcohol; farnesol; Aedes aegypti; mosquito; juvenile hormone; short chain dehydrogenase

INTRODUCTION

Dehydrogenases/reductases are enzymes found across a wide range of organisms, where they perform a broad spectrum of metabolic functions. A classification of short- (SDR), medium- (MDR) and long-chain dehydrogenase/reductases (LDR) has been described based on molecular size, sequence motifs, mechanistic features and structural analysis (Kavanagh et al., 2008; Persson et al., 2009). Common to all three types of oxidoreductases is the occurrence of a Rossmann-fold dinucleotide cofactor motif composed of a central, twisted parallel β-sheet consisting of 6–7 β-strands, which are flanked by 3–4 α-helices from each side (Kavanagh et al., 2008). The three oxidoreductases families share the ability to

Correspondence to: Fernando G. Noriega, Department of Biological Sciences, Florida International Unrversrty, 11200 SW 8th ST. Miami, FL 33199, USA., Telephone: (305)-348-6632., Fax: (305)-348-1986, noriegaf@fiu.edu.
[#]Current address: School of Biological Sciences, University of Queensland, Australia.

The authors do not have a conflict of interest to declare.

interconvert substrates containing hydroxyl/ketone groups, but show distinct chemical mechanisms based on well-defined distinct sequence motifs and domains organizations.

The SDR constitutes one the oldest and largest families of enzymes with over 46,000 members in sequence databases. About 25% of all known dehydrogenases belong to the SDR family. This family is present in archaea, bacteria, and eukaryota, emphasizing their versatility and fundamental importance for metabolic processes (Persson et al., 2009; Kallberg & Persson, 2006; Jörnvall et al., 1999). SDR enzymes have critical roles in lipid, amino acid, carbohydrate, hormone and xenobiotic metabolism as well as in redox sensor mechanisms (Kavanagh et al., 2008). The typical SDR architecture displays one-domain architecture with 250 amino acid length and the substrate binding site located in a highly variable carboxyl-terminal region (Kavanagh et al., 2008).

The best characterized insect SDRs are the alcohol dehydrogenases from *Drosophila* (Atrian et al., 1998; Ashburner, 1998; Benach et al., 1998; Benach et al., 1999; Heinstra, 1993; Sullivan et al., 1990). Two additional groups have been described: 1) a cluster of six *Drosophila* SDRs involved in retinoid metabolism (Belyaeva et al., 2009), and 2) *Jingwei,* a newly evolved SDR gene present only in *Drosophila teissieri* and *Drosophila yakuba,* which is able to oxidize ethanol and long chain alcohols, as well as farnesol and geraniol (Zhang et al., 2004). Recently, Mayoral et al. (2009a) described a $NADP^+$-dependent SDR (AaSDR1) that efficiently oxidizes farnesol into farnesal in the *corpora allata* (CA) of the mosquito *Aedes aegypti.* While the substrate specificity and the biochemistry properties of this enzyme were studied, nothing was known about the additional seven members of a cluster of closed related enzymes.

In the present work, we performed a biochemical and computational modeling characterization of a cluster of eight *aedes aegypti* SDRs (AaSDRs). The 8 AaSDRS are $NADP^+$-dependent, have specific S-enantioselectivity and catalyze secondary alcohols with 8 to 15 carbons; but had diverse substrate specificity. AaSDR1 was the only protein that was able to process isoprenoid alcohols. A structural characterization of AaSDR1, AaSDR4 and AaSDR9 was performed by homology modeling using human SDR as template. The computational study helped to explain the selectivity towards the (10S)-isomers as well as the lower activity of AaSDR4 and AaSDR9 for longer isoprenoid substrates. The current study contributes to the understanding of the structure, expression pattern, biochemical properties and catalytic mode of action of the members of this AaSDRs group.

MATERIALS AND METHODS

Chemicals

(E,E)-farnesol, (Z,Z)-farnesol, (E,E,E)-geranylgeraniol were purchased from Echelon (Salt Lake City, UT). Nerol, citronellol, 1-dodecanol, 2-dodecanol, 2-decanol, R-2-octanol, S-2-butanol, R-2-butanol were purchased from Acros Organics (NJ, USA). Geraniol was purchased from Sigma Aldrich (St Louis, MO). 2-butanol was purchased from MP Biomedicals (Santa Ana, CA). 2-octanol was purchased from Alfa Aesar (Ward Hill, MA).

Insects

Aedes aegypti of the Rockefeller strain were reared at 28°C and 80% relative humidity under a photoperiod of 16h light: 8h dark. Female adults were offered a cotton pad soaked in sucrose 3% solution. We will refer to the cotton wool pad sucrose–fed females as “sugar-fed”.

AaSDRs identification, expression and characterization

AaSDR1 was originally isolated as an expressed sequence tag (EST) from an *A. aegypti* corpora-allata + corpora cardiaca library, constructed and sequenced as previously described (Noriega et al., 2006). The AaSDR1 EST sequence was queried against the *A. aegypti* database at VectorBase (Lawson et al., 2009); it revealed seven additional SDRs with degrees of similarity of 50% or more (AaSDR2: AAEL017320, AaSDR3: AAEL007669, AaSDR4: AAEL017452, AaSDR5: AAEL001461, AaSDR7: AAEL017179, AaSDR8: AAEL010677 and AaSDR9: AAEL010075). The eight *A. aegypti* SDRs cDNAs were PCR-amplified, sequenced and their coding region were cloned into the expression vector pET28a(+) (Novagen, Gibbstown, NJ). *E. coli* strain BL21 (DE3) were transformed with the constructs and expressed as previously described (Mayoral et al., 2009a). Recombinant His-tagged proteins were purified using HisPur™ Cobalt Spin Columns (Pierce, Rockford, IL) as previously described by Mayoral et al. (2009b).

RNA extraction andPCRfor expression analysis

Total RNA was isolated from mosquitoes or tissues using RNA-binding glass powder as previously described (Noriega and Wells, 1993). Contaminating genomic DNA was removed using the DNA-free™ kit (Ambron, Austin, TX). Reverse transcription was carried out using the Reverse-iT™ First Strand Synthesis Kit (ABgene, Epsom, UK). PCR was done using GoTaq® Flexi DNA Polymerase (Promega) using 1 μl of cDNA template in 20 μl reactions. Ten μl were loaded in 1% agarose gels. Ribosomal protein L32 was used as loading control after normalization using quantitative real time PCR. Real-time PCR was performed with a 7300 Real Time PCR System using TaqMan® Gene Expression Assays together with TaqMan® Universal PCR Master Mix (Applied Biosystems, Foster City, CA) as previously described (Nouzova et al., 2011).

Enzyme assays

The enzymatic activities of the recombinant AaSDRs were analyzed using an spectrophotometric assay based on the different optical properties at 340 nm of nicotinamide adenine dinucleotide phosphate ($NADP^+$) and its reduced form (NADPH), as described by Mayoral et al. (2009a). The effect of pH on the activity of the AaSDRs was determined using Stauffer's Buffer (Stauffer, 1989) ranging from 5.0–11.0 and 2-decanol as substrate. The analysis of the effect of metal salts, inhibitors and reducing reagent were performed with and without a pre-incubation time. When a pre-incubation time was included in the protocol, enzyme and inhibitor/stimulator were incubated in half of the total reaction volume for 15 minutes at room temperature (RT) and afterwards the reaction was started with the addition of the rest of the reagents. Control reaction mixtures included the enzymes incubated in the same condition as the treatments but in the absence of any inhibitors/stimulator and results are expressed as percentages of the control values. Reactions were run in triplicate or quadruplicate and three to five independent experiments were carried out for each treatment.

Modeling of AaSDR1, AaSDR4 and AaSDR9

The molecular models of AaSDR1, AaSDR4 and AaSDR9 were built by homology modeling using Modellers (Eswar et al., 2008; Sali and Blundell, 1993) and the crystal structure of human SDR (uniprot-Q6UWP2) (PDB ID: 1XG5). Assessments of the reliability of the models was carried out using PHYRE (Kelley and Sternberg, 2009) and WHAT_CHECK (Hooft *et al.,* 1996) as previously described (Defelipe et al., 2011). Structural alignment and visualization were done with the program VMD (Eargle *et al.,* 2006; Humphrey *et al.,* 1996). Images were rendered with Tachyon (Stone, 1998).

Docking experiments

Docking simulations were carried out using the program Autodock4 (Morris *et al.,* 2009). We used the Lamarckian genetic algorithm for the conformational searches. The following parameters were used for all the simulations: a population size of 300 individuals, 7.5 million energy evaluations, mutation rates of 0.02, crossover rate of 0.8 and an elitism value of 1. For each ligand, 250 independent docking runs were performed and results differing by less than 0.5 Å were clustered together. To validate our docking protocol, $NADP^+$ was removed from the model and docked again. Afterwards, wrth $NADP^+$ located in the active she, we performed the docking of the substrates (E,E)-farnesol, (Z,Z)-farnesol, (2S)-octanol and (2R)-octanol. To reduce conformational heterogeneity, proteins were kept rigid throughout these runs and docking experiments were performed with an added potential of 1 kcal/mol $Å^2$ on the alcohol oxygen atom in the position expected for catalysis.

Phylogenetic analysis

SDR sequences were obtained from GenBank and VectorBase databases and used for the alignments and phylogenetic analysis using Phylogeny.fr as previously described (Mayoral et al. 2009a).

Statistical Analysis

Statistical analysis of the data was performed by t test using GraphPad Prism version 3.00 for Windows (Graphpad Software, San Diego, CA). The results were expressed as mean ± SD and considered significantly different at $P < 0.05$.

RESULTS

Insect's SDR clusters

A group of eight SDRs that shared at least 50% similarity were found in the *A. aegypti* genome. Important residues that characterize them as members of one of the three NADPH-dependent subfamilies, the cP2 SDR subfamily (Kallberg et al., 2002), were well conserved (Fig. 1). The glycine-rich TGxxxGxG motif essential for coenzyme binding was present in every insect's SDRs analyzed. Sequence alignments and structural models helped to identify several critical residues: 1) Ala_{92}, Thr_{197}, Gly_{193} and Pro_{192} are involved in interactions wrth the cofactor $NADP^+$, and 2) Ser_{145}, Tyr_{160} and Lys_{164} are members of the catalytic triad (Fig. 1).

Similar clusters of related SDRs were detected in other species of Diptera; ten sequences in *Culex pipiens,* six SDRs in the *Anopheles gambiae* genome and six *Drosophila melanogaster* SDRs (Fig. 2). Related SDR clusters were also found in Coleoptera (7 *Tribolium castaneum* genes) and Hemiptera (3 *Acyrthosiphon pisum* SDRs). On the contrary, only one orthologue was found for *Nasonia vitripennis, Apis mellifera* and *Pediculus humanus* (Fig. 2). To further understand the evolution of these SDRs clusters, we analyzed the presence and distribution of introns. All insect SDRs examined share an intron in the same position (Supplementary Fig. 1), between the well conserved amino acids Thr_{188} and Ser_{189} (Fig. 1). This conserved intron position suggests that all the SDRs included in our study originally evolved from a single ancestor, duplicated and diversified independently from each other. Among dipterans, three genes had a second intron (one in *Aedes, Culex* and *Drosophila)* and their positions are also well conserved (Supplementary Fig. 1). SDR genes in Coleoptera and Hemiptera also have this second intron in exactly the same location. In addition, all the species of *Tribolium* had a third intron.

In *Anopheles gambiae* the 6 SDR genes cluster together in the chromosome region 2L; *Drosophila melanogaster* 6 genes are also clustered in the same chromosome region. The

sequences of *Culex pipiens* group into two clusters. One contains six paralogues and the other contains five, suggesting that the group with five paralogues aroused out of a duplication-inversion event of the original cluster (Supplementary Fig. 1).

AaSDRs developmental expression and tissue specificity

There were distinct differences in the expression of the 8 AaSDRs during mosquito life cycle (Table 1). Most AaSDRs showed the highest overall expression in adults; the exceptions were AaSDR4 that was expressed only in the larvae and AaSDR5 that was not transcribed at any stage and consequently was not further studied.

AaSDR1, AaSDR2 and AaSDR9 were the SDRs with highest levels of expression in the adult female mosquito (Fig. 3). AaSDR1 and AaSDR9 were highly expressed in midgut, fat body and brain, with lower expression in Malpighian tubules and ovaries. AaSDR7 had a strong and specific expression in the ovaries. AaSDR9, AaSDR1, AaSDR7 and AaSDR4 were expressed in the testes. We detected the presence of AaSDR1, AaSDR8, and AaSDR9 transcripts in the CA, but only AaSDR1 and AaSDR9 had relatively high level of expression, and only AaSDR1 increased its expression in the CA from 0 to 24h after emergence, in synchrony with the synthesis of JH in this gland (Supplementary Fig. 2).

Biochemical characterization of the AaSDR cluster

The calculated molecular mass size of the recombinant AaSDR monomers ranged from 28.5–29.6 kDa (including the His-tag). AaSDR2 and AaSDR8 presented additional forms, suggesting they aggregate as dimers and multimers (Supplementary Fig. 3). The presence of recombinant monomers and multimers was confirmed using an anti-His tag antibody (Supplementary Fig. 3). The enzymatic activity of all the AaSDRs increased on alkalinity conditions, reaching an optimum at pH 10.0 (Fig. 4). The substrate specificities of the AaSDR cluster members were studied testing several types of alcohols (isoprenoids, primary or secondary alcohols) with different chain lengths. The levels of activity and substrate specificities of the seven AaSDR enzymes were different (Table 2A). AaSDR1, AaSDR2 and AaSDR9 were the most active enzymes, efficiently processing alcohols ranging from 8 to 15 carbons, with higher catalytic activity on alcohols with 10 to 12 carbons. In addition, AaSDR1 effectively oxidized isoprenoid alcohols; AaSDR2 and AaSDR9 also oxidized farnesol and nerol, but at approximately 10 times lower rate than AaSDR1. With relatively low efficiency, AaSDR3, AaSDR4, AaSDR? and AaSDR8 also showed preference for alcohols with 8 to 15 carbons. Independent of the chain-length, most SDRs analyzed had strong preference for the secondary aliphatic alcohols; *e.g.* AaSDR9 was 70 fold more active on 2-dodecanol than 1-dodecanol; and 50 fold more active on 2-octanol than 1-octanol. Similar results were obtained for additional members of the AaSDR cluster. The AaSDRs with higher enzymatic activities had a clear enantio-specificity for the S-forms when 2-octanol and 2-butanol were used as substrates (Table 2B).

We also evaluated the effect on the activity of AaSDR1 and AaSDR8 of the alkylating agent iodoacetamide, metal salts such as $ZnCl_2$, $CuCl_2$ and $MgCl_2$, chelating agents such as EDTA, and reducing agents such as β-mercaptoethanol and dithiothreitol (DTT) (Table 3A). Overall, $CuCl_2$ and $ZnCl_2$ had strong inhibitory effects, while addition of DDT increased enzymatic activity (Table 3A). When we pre-incubated these enzymes with the inhibitors/stimulators for 15 minutes at RT prior the assay, their effects were similar but more accentuated than when no pre-incubation was step was included (Table 3B).

Modeling AaSDR structures and docking of potential substrates

The AaSDR1 structure obtained by homology modeling had the typical Rossmann-fold motif of oxireductases composed by a central twisted parallel β-sheet of seven β-strands

flanked by three α-helices on each side (Supplementary Fig. 4). In order to characterize the active site $NADP^+$ and (E,E)-farnesol were docked into the apo-structure of AaSDR1. We identified hydrogen bonds between the protein and the ligand (hydrogen donor groups were between 4 Å of hydrogen acceptor groups and the angle between the hydrogen and the heavy atoms were 180° +/− 30°). $NADP^+$-protein interactions are provided by 3 specific hydrogen bonds: one between the Thr_{197}alcohol group and the carbonyl oxygen of the nicotinamide ring, the second is formed between the amide group of the nicotinamide ring and the carbonyl oxygen of Gly_{193} and the third is formed between Ala_{92} and one of the alcohol groups of the sugar. In addition Pro_{192} contributes to the placement of $NADP^+$ inside the active site by interacting with the nicotinamide ring (Supplementary Fig. 5).

The catalytic activity of AaSDR1 includes the deprotonation of the alcohol group of the substrate and the subsequent abstraction of a hydride from the carbonyl carbon that is transferred to the $NADP^+$ cofactor producing NADPH and the oxidized product. In the case of AaSDRs we propose that a negative charged Tyr_{160} is involved in the abstraction of the proton from the donor alcohol (Fig. 5). The positively charged Lys_{164} is essential to stabilize the negative Tyr_{160} (Fig. 6). The last component of the catalytic triad is Ser_{145} that forms a hydrogen bond with the oxygen of the alcohol group of the substrate to be oxidized (Fig. 5 and Fig. 6).

The high stereo-selectivity of AaSDR1 for S-2-octanol could be explained using our 3D-model (Fig. 7). When the 2S-conformer is docked in the active site, the hydride donor carbon is positioned in a conformation were the hydrogen atom can be transferred to the nicotinamide ring of $NADP^+$ and the long aliphatic chain of octanol is correctly docked in the hydrophobic pocket of the protein. However, when the 2R-conformer is docked in the active site, the hydrogen atom cannot be positioned in a suitable conformation for catalysis if the aliphatic chain goes inside the hydrophobic pocket; this may explain the reduced catalytic activity for the 2R-isomer (Fig. 7).

In order to understand the biochemical behavior observed among the different proteins of the AaSDR cluster, we also modeled the structures of AaSDR4 and AaSDR9 Structural alignment of the 3 models showed that the overall fold is well conserved among the three AaSDRs (Supplementary Fig. 6). However, AaSDR1 had a large active site able to accommodate (E,E)-farnesol, the other 2 enzymes had smaller pockets that may not be able to accommodate long-chain substrates such as (E,E)-farnesol (Fig. 8). We also observed that cysteines Cys_{63} and Cys_{123}, which are well conserved in all the AaSDR, were close enough to form a disulfide bond in the proximity of the active site (Supplementary Fig. 7).

DISCUSSION

Evolution of an insect SDR cluster

SDR enzymes have critical roles in lipid, amino acid, carbohydrate, hormone and xenobiotic metabolism as well as in redox sensor mechanisms (Kavanagh et al., 2008). A Position-Specific Itinerated Blast (PSI-Blast) analysis revealed orthologues to members of the AaSDRs cluster among diverse taxa (Supplementary Fig. 8). The biological functions of most of the members of these clusters of enzymes are not defined or experimentally confirmed. That makes it difficult to determine an ancestral gene from which the AaSDRs cluster of enzymes could have been originated.

Similar clusters of cP2 SDRs were found in a diverse group of insects and in most cases paralogues for each species had higher sequence similarity with each other than when compared with orthologue SDRs in other insect species (Fig. 2). This indicates that these SDR gene duplications and diversifications occurred independently and frequently during

insect evolution and suggest that some physiological advantage is associated with these duplication events.

Structural and biochemical properties of the AaSDRs

Critical motifs important for coenzyme binding and catalysis were well conserved in every insect SDRs analyzed. Previous studies suggest that the Tyr_{160} acts as the catalytic base, whereas Ser_{145} stabilizes the substrate and Lys_{164} interacts with the nicotinamide ribose and decreases the pKa of the Tyr-OH moiety (Oppermann et al., 2003). The optimal pH for all AaSDRs was close to 10.0, consistent with the notion that an ionized Tyr_{160} (pK=10) is involved in catalysis. Similar pH dependence has been observed in other enzymes of the group (Winberg et al., 1986; Zhang et al., 2010). Oppermann et al. (2003) suggested that the Asn_{116} is also part of the SDR's active site, forming a tetrad with the 3 residues already described. Asn_{116} is conserved among all AaSRDs, as well as in 45 of 46 SDR sequences analyzed in the present study. The *Drosophila* ADH structure revealed interactions of this conserved Asn_{116} residue with the active site Lys_{164} via a water molecule (Beneach et al., 1998). The essential role of this residue was also established by mutational and structural analysis using bacterial 3B/17B/-HSD as a model system (Filling et al., 2002). In our comparative models Asn_{115} could be interacting directly or water mediated with Lys_{164}, emphasizing the idea of a catalytic role for this residue. Cysteines Cys_{63} and Cys_{123} are well conserved in all the AaSDRs, as well as in all the insect SDRs analyzed. Their thiol groups are facing each other indicating that they could form a disulfide bond. Due to their proximity to the catalytic pocket they could play an important role in the stabilization of the pocket. Iodoacetamide, which binds covalently to the thiol group of cysteines, causes a significant inhibition of AaSDRs activities; suggesting that these cysteine residues are important for optimal enzyme catalysis. A similar inhibitory effect was observed on a SDR from *Sulfolobus acidocaldarius* (Pennacchio et al., 2010). We also noticed a positive correlation between the number of cysteines on AaSDR1 and AaSDR8 (2 *vs.* 4) and the increasing effect of DTT on enzymatic activities. The structural models could not predict the formation of a second disulfide bond with another pair of cysteines since they are located in opposite sides of the protein, facing the solvent.

Most SDRs have been described as dimers or tetramers (Jörnvall et al., 1995). SDRs dimerization interfaces have been described across two perpendicular two fold axes, involving a four-helix bundle and a β-sheet that extends across two subunits (Kavanagh et al., 2008). The additional thiol groups present in AaSDR8 (2 extra Cys) and AaSDR2 (1 extra Cys) might be involved in a dimerization process and could explain the higher propensity of AaSDR8 and AaSDR2 to aggregate. The enzymatic activity of AaSDR8 was stimulated by the addition of a relatively low amount of DTT or mercaptoethanol, suggesting a dissociation of inactive multimers or the disruption of protein aggregation.

SDRs are not recognized to be metal dependent enzymes; however, the *Lactobacillus brevis* cP2 alcohol dehydrogenase exhibited a strong Mg^{2+} dependency (Niefind et al., 2003; Pennaachio et al., 2010). The crystallographic analysis revealed that each tetramer contains two magnesium ions, although the metal was not considered a direct catalytic cofactor (Niefmd et al., 2003). We found only a moderate effect of Zn^{+2} and Cu^{+2} on AaSDRs activities; tins mild effect, together with the inhibition by iodoacetamide, suggests that these compounds could be reacting with the –SH groups of cysteines and ultimately affecting the tertiary and quaternary structure of the protein. Similar inhibitory/stimulatory results were reported on the activity of the 7α-hydroxysteroid dehydrogenase of *E coli* (Prabha et al., 1989), as well as on the tetrameric NAD(H)-dependent dehydrogenase from *Sulfolobus acidocaldarius* (Pennacchio et al., 2010). Additional studies will be necessary to confirm and further understand the effect of metal ions on SDRs activities.

SDRs functions in insects

The *Drosophila* alcohol dehydrogenase (DADH) is the most extensively studied SDR group in insects. DADHs cannot process long chain alcohols and show preference for short alcohols such as ethanol. In contrast, our studies revealed that all AaSDRs have a strong preference for long chain secondary alcohols over short chain primary alcohols, with none of the enzymes accepting ethanol as a substrate. Stereospecificity assays revealed that AaSDRs have strong preference for S-isomers. These results support the hypothesis that SDRs enzymes are pro-S, whereas the metal dependent medium-chain ADH are pro-R (Schenider-Bernlohr et al., 1986). Structural studies on alcohol dehydrogenases from *Saccharomyces cerevisiae* and *Lactobacillus brevis* described that the stereo-selectivity of the reaction center had no correlation with the presence/absence of metal, the use of NADH or NADPH as cofactor or the size of the substrate that can be accepted (Kwiecien et al., 2009). The stereo-selectivity is probably defined by the geometry of the active site (Kwiecien *et al.*, 2009). In the docking and molecular structure studies we found that the S conformation allowed interactions with the 2C of the substrate and permit transference of hydrogen to the nicotinamide ring of $NADP^+$; in contrast the hydrogen in the R-substrate is feeing the opposite direction and prevents the interaction with the $NADP^+$ ring.

Drosophila alcohol dehydrogenase oxidizes alcohols to aldehyde/ketones, both for detoxification and for metabolic purposes. A small number of alcohol dehydrogenases closely related to DADH have been studied in *Sarcophaga peregrina* (Matsumoto et al., 1995; Horio et al., 1996), *Ceratitis capitata* and *Bactrocera oleae* (Brogna et al., 2001). It has been hypothesized that DADH have evolved as an adaptation to *Drosophila* feeding behavior and the use of fermenting substrates as breeding sites (Lachaise et al., 1988; Geer et al. 1985; Ashburner, 1998). However, while *Sarcophaga* fed excrement, decaying vegetable or animal matter and does not live in ethanol-rich environments, the pattern of expression of ADH is almost identical to that of the DADH gene (Horio et al., 1996).

In situ distribution studies of the alcohol dehydrogenase in *Drosophila* larvae showed strong expression in fat body and alimentary tract. In the oxidation of ethanol, NAD^+ is needed to generate acetaldehyde and NADH. The ADH enzyme is involved in the *in vivo* conversion of the acetaldehyde into acetate in larvae, whereas the aldehyde dehydrogenase enzyme is responsible for this conversion in adults (Heinstra 1993). AaSDRs and DADH sequence similarities were below 20%, suggesting these two groups of SDRs diverged long time ago and evolved separately under different selective pressures. AaSDRs have a more complex expression pattern than the DADH; each enzyme of the cluster had a different pattern of expression suggesting that they evolved to have different function in different tissues. Alcohol dehydrogenases are known for being specific to a narrow range of small substrates (Sofer and Ursprung, 1968); in contrast, AaSDRs oxidized 8–12 carbon secondary alcohols, with preference for 10 carbon alcohols. In addition of these substrates, AaSDR1 efficiently processed isoprenoid substrates and plays a role in JH synthesis; the functions in other tissues other than the CA are presently unknown and need further studies.

An enzyme with similar substrate specificity to AaSDR1 has been recently reported; *Jingwei* is a chimeric gene that appeared 2.5 million years ago in the common ancestor of two African *Drosophila* species, *D. yakuva* and *D. teissieri* (Zhang *et al.,* 2004; 2010). *Jingwei* efficiently utilizes long-chain primary and secondary alcohols (including geraniol and farnesol). It is remarkable that while AaSDR1 and *Jingwei* have the capability of using farnesol or geraniol as substrate, the similarity between them at the amino acid level is only 15%. However, while *Jingwei* can still process ethanol and primary alcohols (Zhang *et al.,* 2004), AaSDRs have lost the ability to process short alcohols like ethanol.

AaSDRs and JH synthesis

JHs are key hormones involved in the regulation of insect development and reproduction (Goodman and Granger, 2005). The early steps of JH III biosynthesis follow the mevalonate pathway to form farnesyl pyrophosphate (FPP) (Belles *et al.,* 2005). During the late steps, FPP is transformed sequentially to farnesol, farnesal, farnesoic acid, methyl farneosate and JH III (Belles *et al.,* 2005). Mayoral et al. (2009a) reported the identification of AaSDR1 in the CA of mosquitoes as a putative candidate for the oxidation of farnesol into farnesal in the JH synthesis pathway. In this work we further characterized the whole AaSDRs cluster and tested if any additional cluster member could play a role on JH synthesis. Only AaSDR1 and AaSDR9 are highly expressed in the CA 24h after adult eclosion during the peak of JH synthesis (Li et al., 2003). While AaSDR8 is transcribed in low levels, the other members of the cluster are not expressed in the CA at this critical time. The expression pattern of AaSDR1 mRNA during the mosquito development also correlates well with the rates of JH synthesis in mosquitoes (Mayoral et al., 2009a). After testing all the AaSDRs against a broad range of substrates, only AaSDR1 was able to efficiently oxidaze (E,E)-Farnesol, the natural precursor of JH. The simulated docking scores for (E,E)-Farnesol were significantly better ($K_{binding}$ = 38.76 μM) than those for (Z,Z)-Farnesol ($K_{binding}$ = 88.91 μM). AaSDR9 and AaSDR2 had slight preference for the (Z) isomers. The general structure and folds of the 3 protein models were similar, although there were differences in the flexible parts. The active site volume of AaSDR1 was significantly larger than those of the other two AaSDRs, Those differences could be explained by a smaller catalytic pocket in AaSDR4 and AaSDR9 created by several changes: the change of Leu_{201} for a Phe in AeSDR9, the change of Val_{194} for a Met in AaSDR4 and the substitution of Ser_{158} for a Leu in AaSDR4 and a Tyr in AaSDR9. These changes might explain why AaSDR1 is able to accommodate (E,E)-Farnesol, while AaSDR4 and AaSDR9 would have more trouble fitting the long isoprenoid chain.

In summary, we identified a cluster of eight closely related cP2 AaSDRs in mosquitoes. They are all NADP+-dependent enzymes with S-enantioselectivity and preference for secondary alcohols with 8–15 carbons. Members of the cluster differ on tissue specificity and developmental expression. Molecular, biochemical and modeling studies support the hypothesis that AaSDR1 is the only member of the cluster involved in JH synthesis in the CA of mosquitoes. Our studies provide insight into the structural features that influence the catalytic flexibility of different short chain dehydrogenases.

Supplementary Material

Refer to Web version on PubMed Central for supplementary material.

Acknowledgments

We would like to thank Crisalejandra Rivera-Perez and Mario Perez for critical reading and feedback on the manuscript. This work was supported by NIH Grant AI 45545 to F.GN. This work was partially supported by grants from Universidad de Buenos Aires and ANPCYT to AT. AT is a member of CONICET.

LITERATURE CITED

Ashburner M. Speculations on the subject of alcohol dehydrogenase and its properties in Drosophila and other flies. BioEssays. 1998; 20:949–954. [PubMed: 9872061]

Atrian S, Sanchez-Pulido L, Gonzalez-Duarte R, Valencia A. Shaping of *Drosophila* alcohol dehydrogenase through evolution: relationship with enzyme functionality. J Mol Evol. 1998; 47:211–221. [PubMed: 9694670]

Belyaeva OV, Lee S-A, Kolupaev OV, Kedishvili NY. Identification and Characterization of Retinoid-Active Short-Chain Dehydrogenases/Reductases in Drosophila melanogaster. Biochim Biophys Acta. 2009; 1790:1266–1273. [PubMed: 19520149]

Bellés X, Martin D, Piulachs M-D. The mevalonate pathway and the synthesis of juvenile hormone in insects. Ann Rev Entomol. 2005; 50:181–190. [PubMed: 15355237]

Benach J, Atrian S, Gonzalez-Duarte R, Ladenstein R. The refined crystal strucutre of Drosophila lebanonensis alcohol dehydrogenase at 1.9 resolution. J Mol Biol. 1998; 282:383–399. [PubMed: 9735295]

Benach J, Atrian S, Gonzalez-Duarte R. The catalytic reaction and inhibition mechanism of Drosophila alcohol dehygrogenase: observation of an enzyme-bound NAD-ketone adduct at 1.4 resolution by X-ray crystallograpgy. J Mol Biol. 1999; 289:335–355. [PubMed: 10366509]

Brogna S, Benos PV, Gasperi G, Savakis C, Grant BR, Klein J. The Drosophila alcohol dehydrogenase gene may have evolved independently of the functionally homologous medfly, olive fly, and flesh fly genes. Mol Biol Evol. 2001; 18:322–329. [PubMed: 11230533]

Eargle J, Wright D, Luthey-Schulten Z. Multiple Alignments of protein structures and sequences for VMD. Bioinformatics. 2006; 22:504–506. [PubMed: 16339280]

Eswar N, Eramian D, Webb B, Shen MY, Sali A. Protein structuremodeling with MODELLER. Methods Mol Biol. 2008; 426:145–159. [PubMed: 18542861]

Filling C, Berndt KD, Benach J, Knapp S, Prozorovski T, Nordling E, Ladenstein R, Jornvall H, Oppermann U. Critical residues for structure and catalysis in short-chain dehydrogenases/reductases. J Biol Chem. 2002; 277:25677–25684. [PubMed: 11976334]

Geer BW, Langevin ML, McKechnie SW. Dietary ethanol and lipid synthesis in *Drosophila melanogaster*. Biochem Genet. 1985; 23:607–22. [PubMed: 2932099]

Goodman, W.; Granger, N. The juvenile hormones. In: Gilbert, LI.; Iatrou, K.; Gill, SS., editors. Comprehensive molecular insect science. Vol. 3. Oxford: Elsevier Pergamon; 2005. p. 319-408.

Jörnvall H, Persson B, Krook M, Atrian S, Gonzalez-Duarte R, Jeffery J, Ghosh D. Short Chain Dehydrogenase/Reductases (SDR). Biochemistry. 1995; 34:6003–6013. [PubMed: 7742302]

Jörnvall H, Hoog J-O, Persson B. SDR and MDR: completed genome sequences show these protein families to be large, old origin, and of complex nature. FEBS Lett. 1999; 445:261–264. [PubMed: 10094468]

Heinstra PWH. Evolutionary genetics of the *Drosophila* alcohol dehydrogenase gene-enzyme system. Genetica. 1993; 92:1–22. [PubMed: 8163153]

Hooft RW, Vriend G, Sander C, Abola EE. Errors in protein structures. Nature. 1996; 381:272. [PubMed: 8692262]

Horio T, Kubo T, Natori S. Purification and cDNA cloning of the alcohol dehydrogenase of the flesh fly Sarcophaga peregrina. Eur J Biochem. 1996; 237:698–703. [PubMed: 8647115]

Kallberg Y, Oppermann U, Jornvall H, Persson B. Short-chain dehydrogenases/reductases (SDRs). Coenzyme-based functional assignments in completed genomes. Eur J Biochem. 2002; 269:4409–4417. [PubMed: 12230552]

Kallberg Y, Persson B. Prediction of coenzyme specificity in dehydrogenases/reductases: a hidden Markov model-based method and its application on complete genomes. FEBS J. 2006; 273:1177–1184. [PubMed: 16519683]

Kavanagh KL, Jornvall H, Persson B, Opperman U. The SDR superfamily: functional and structural diversity within a family of metabolic and regulatory enzymes. Cell Mol Life Sci. 2008; 65:3895–3906. [PubMed: 19011750]

Kelley LA, Sternberg MJE. Protein structure prediction on the Web: a case study using the Phyre server. Nature Protocols. 2009; 4:363–371.

Kwiecien RA, Ayadi F, Nemmaoui Y, Silvestre V, Zhang B-L, Robins RJ. Probing stereoselectivity and pro-chirality of hydride transfer during short-chain alcohol dehydrogenase activity: A combined quantitative ^{2}H NMR and computational approach. Arch Bxochem Bxophys. 2009; 482:42–51.

Lachaise D, Cariou ML, David JR, Lemeunier F, Tsacas L, Ashburner M. Historical biogeography of the Drosophila melanogaster species subgroup. Evol Biol. 1988; 22:159–225.

Lawson D, Arensburger P, Atkinson P, Besansky NJ, Bruggner RV, Butler R, et al. VectorBase: a data resource for invertebrate vector genomics. Nucleic Acids Res. 2009; 37:583–587.

Li YP, Hernandez-Martinez S, Unnithan GC, Feyereisen R, Noriega FG. Activity of the corpora allata of adult female *Aedes aegypti*: effects of mating and feeding. Insect Biochem Mol Biol. 2003; 33:1307–1315. [PubMed: 14599502]

Mayoral JG, Nouzova M, Navare A, Noriega FG. NADP+-dependent farnesol dehydrogenase, a corpora allata enzyme involved in juvenile hormone synthesis. Proc Natl Acad Sci USA. 2009a; 106:21091–21096. [PubMed: 19940247]

Mayoral JG, Nouzova M, Yoshiyama M, Shinoda T, Hernandez-Martinez S, Dolghih E, Turjanski AG, Roitberg AR, Priestap H, Perez M, Mackenzie L, Li Y, Noriega FG. Molecular and functional characterization of a juvenile hormone acid methyltransferase expressed in the corpora allata of mosquitoes. Insect Bioch Mol Biol. 2009b; 39:31–37.

Matsumoto N, Sekimizu K, Soma G-I, Ohmura Y, Andoh T, Nakanishi Y, Obinata M, Natori S. Structural analysis of a developmentally regulated 25KDa protein gene of *Sarcophaga peregrina*. J Biochem. 1985; 97:1501–1508. [PubMed: 2993269]

Morris GM, Huey R, Lindstrom W, Sanner MF, Belew RK, Goodsell DS, Olson AJ. AutoDock4 and AutoDockTools4: automated docking with selective receptor flexibility. J Comput Chem. 2009; 30:2785–2791. [PubMed: 19399780]

Niefind K, Müller J, Riebel B, Hummel W, Schomburg D. The crystal structure of r-specific alcohol dehydrogenase from *Lactobacillus brevis* suggests the structural basis of its metal dependency. J Mol Biol. 2003; 327:317–328. [PubMed: 12628239]

Noriega FG, Wells MA. A comparison of three methods for isolating RNA from mosquitoes. Insect Molec Biol. 1993; 2:21–24. [PubMed: 9087539]

Noriega FG, Ribeiro JMC, Koener JF, Valenzuela JG, Hernandez-Martinez S, Pham VM, Feyereisen R. Comparative genomics of insect juvenile hormone biosynthesis. Insect Biochem Mol Biol. 2006; 36:366–374. [PubMed: 16551550]

Nouzova M, Edwards M, Mayoral JG, Noriega FG. A coordinated expression of biosynthetic enzymes controls the flux of juvenile hormone precursors in the corpora allata of mosquitoes. Insect BiochemMolec Biol. 2011; 41:660–669.

Pennacchio A, Assunta Giordano A, Pucci B, Rossi M, Raia AC. Biochemical characterization of a recombinant short-chain NAD(H)-dependent dehydrogenase/reductase from *Sulfolobm acidocaldarius*. Extremophiles. 2010; 14:193–204. [PubMed: 20049620]

Persson P, Kallberga Y, Brayd JE, Bruforde E, Dellaportaf SL, Faviag SD, Duarteh RG, Jornvall H, Kavanaghd KL, Kedishvili N, Kisiela M, Maserk E, Mindnichl R, Orchardg S, Penningl TM, Thorntong JM, Adamskim J, Oppermannd J. The SDR (short-chain dehydrogenase/reductase and related enzymes) nomenclature initiative. Chemico-Biological Interactions. 2009; 178:94–98. [PubMed: 19027726]

Oppermann U, Filling C, Huh M, Shafqat N, Wu X, Lindh M, Shafqat J, Nordling E, Kallberg Y, Persson B, Jornvall H. Short-chain dehydrogenases/reductases (SDR): the 2002 update. Chemico-Biological Interactions. 2003; 143/144:247–253. [PubMed: 12604210]

Prabha V, Gupta M, Gupta KG. Kinetic properties of 7α-hydroxysteoid dehydrogenase from *Escherichia coli* 080. Canadian Journal of Microbiology. 1989; 35:1076–1080. [PubMed: 2698265]

Sali A, Blundell TL. Comparative protein modelling by satisfaction of spatial restraints. J Mol Biol. 1993; 234:779–815. [PubMed: 8254673]

Schneider-Bernlohr H, Adolph H-W, Zeppezauer M. Coenzyme Stereospecificity of Alcohol/Polyol Dehydrogenases: Conservation of Protein Types vs. Functional Constraints. J Am ChemSoc. 1986; 108:5573–5576.

Stauffer, C. Enzyme assays for food scientists. Chapman and Hall; New York: 1989. p. 61-76.

Stone, J. Master Thesis. Computer Science Department, University of Missouri-Rolla; 1998. An Efficient Library for Parallel Ray Tracing and Animation.

Sullivan, DT.; Atkinson, PW.; Starmer, WT. Molecular evolution of the alcohol dehydrogenase genes in the genus *Drosophila*.. In: Hecht, M.; Wallace, B.; Prance, G., editors. Evolutionary Biology. Plenum Press; London, UK: 1990. p. 107-147.

Winberg JO, Hovik R, Mckinley-McKee JS, Juan E, Gonzalez-Duarte R. Biochemical properties of alcohol dehydrogenase from *Drosophila lebanonensis*. Journal of Biochemistry. 1986; 235:481–490.

Zhang J, Dean AM, Brunet F, Long M. Evolving protein functional diversity in new genes of *Drosophila.* PNAS. 2004; 101:16246–16250. [PubMed: 15534206]

Zhang J, Yang H, Long M, Li L, Dean AM. Evolution of Enzymatic Activities of Testis-Specific Short-Chain Dehydrogenase/Reductase *in Drosophila*. J Mol Evol. 2010; 71:241–249. [PubMed: 20809353]

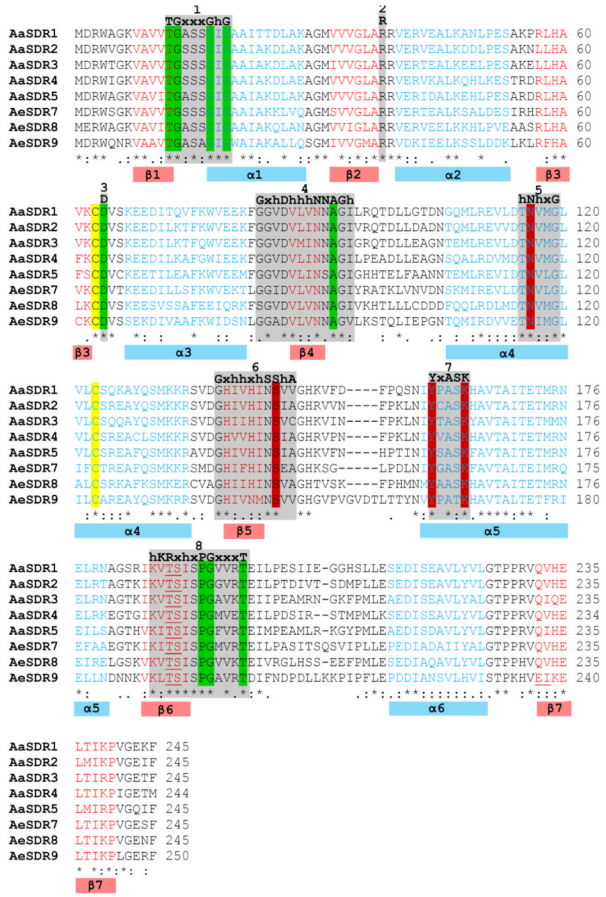

Figure 1. Multiple alignments of the AaSDRs amiuo acid (AA) sequences

Highlighted residues: (1) in red are AA involved in substrate recognition and catalytic activity, (2) in green are AA involved in interactions with the cofactor, (3) in yellow are cysteines forming disulfide bonds and (4) underlined are AA marking the positions of introns. Motifs: (1) Alpha-helices are colored in blue and β-sheets in red and (2) Additional SDR conserved motifs are marked by colored boxes and numbers.

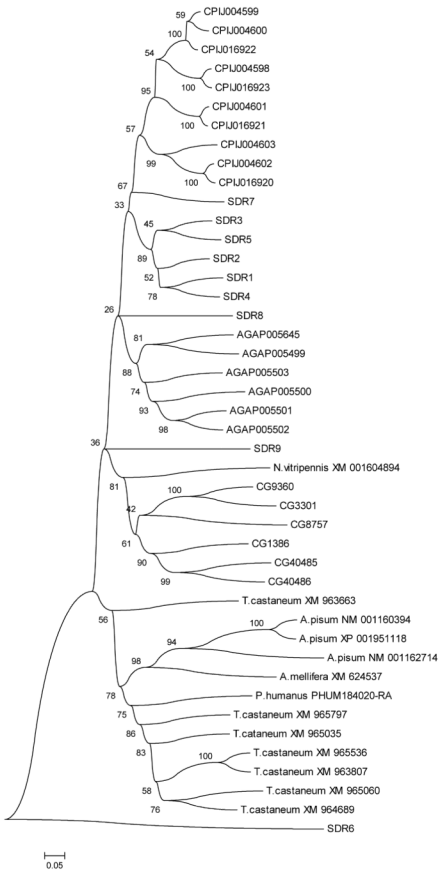

Figure 2. Phylogenetic analysis of SDRs from differences insects based on amino acid sequences

Sequences are labeled with the species names (or acronyms) and accession numbers. SDR: *A. aegypti;* AGA: *A gambiae;* CPUJ: *Culex quinquefasciatus;* T. castaneum: *Tribolium castaneum;* CG: *Drosophila melanogaster;* N. vitripennis: *Nasonia vitripennis;* A. Pisum: *Acyrthosiphonpisum;* A. mellifera: *Apis mellifera.* Accession numbers for AaSRDs are included in materials and methods. AaSDR6 (AAEL002901) has 14% similarity with AaSDR1 and was included in the analysis as an outgroup.

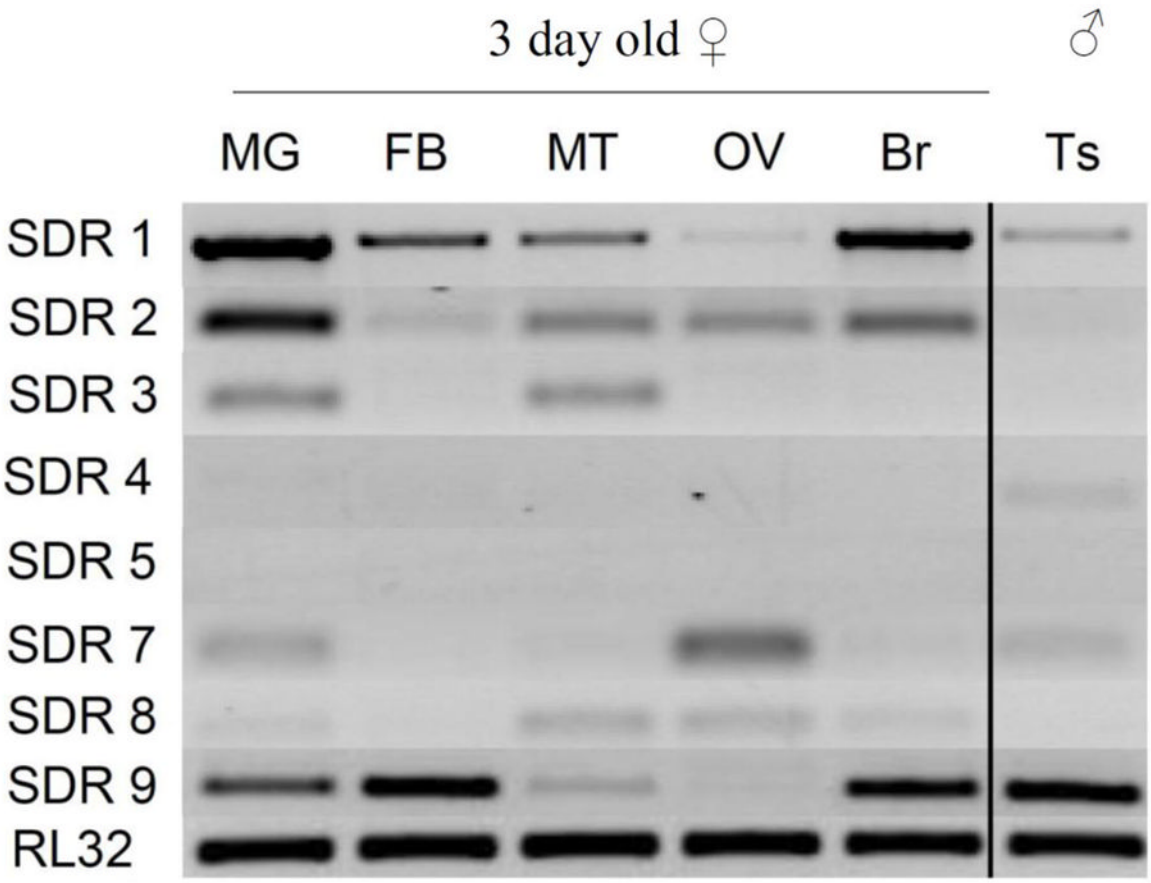

Figure 3. Tissue specific expression of AaSRDs mRNA in adult mosquitoes

PCR amplification of AaSRDs mRNA from adult tissues. All tissues were dissected from 3 days old sugar-fed female mosquitoes; except for the testis, dissected from 3 days old sugar-fed males. MG: midgut, FB: fat body, MT: Malpigian tubules, OV: ovaries, Br: brain. Ts: testis. Ribosomal protein L32 was used as loading control (RL32).

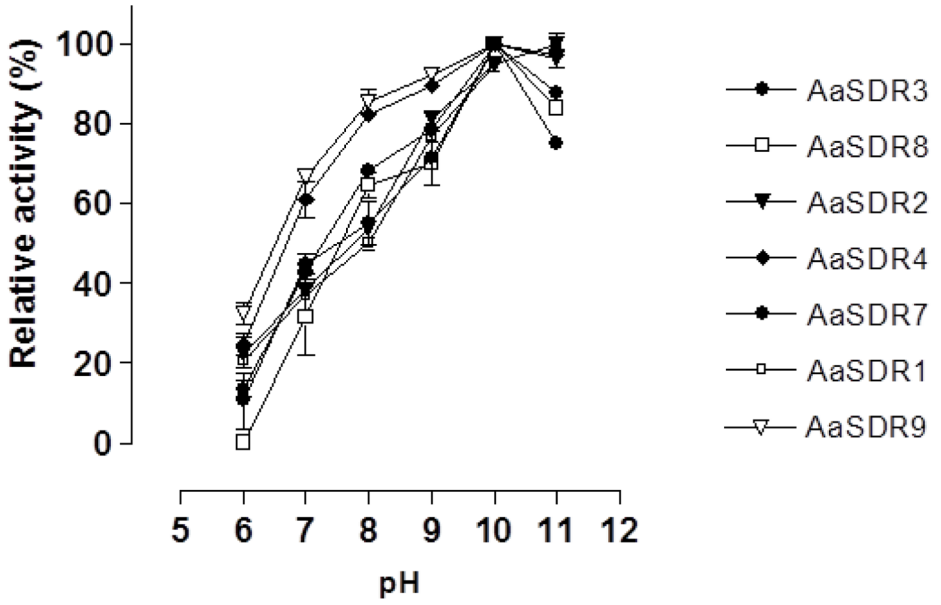

Figure 4. Effect of pH on the activity of the AaSDRs members

The assay was carried out using Stauffer's Buffer pH 5.0–11.0, 2 mM NADP+ and 150 μM of 2-decanol as a substrate. Results are the average of three independent experiments in triplicate.

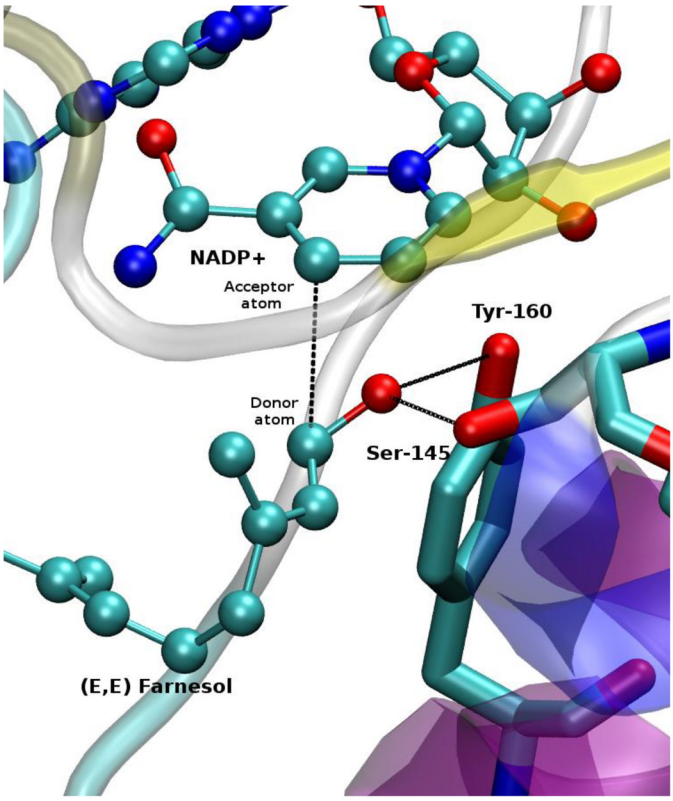

Figure 5. Model of the AaSDR1 active site

Active site of AaSDRs showing a negative charged Tyrl60 involved in the abstraction of the proton from the donor alcohol. The positively charged Lysl64 is essential to stabilize the negative Tyrl60. The last component of the catalytic triad is Serl45 that forms a hydrogen bond with the oxygen of the alcohol group of the substrate to be oxidized.

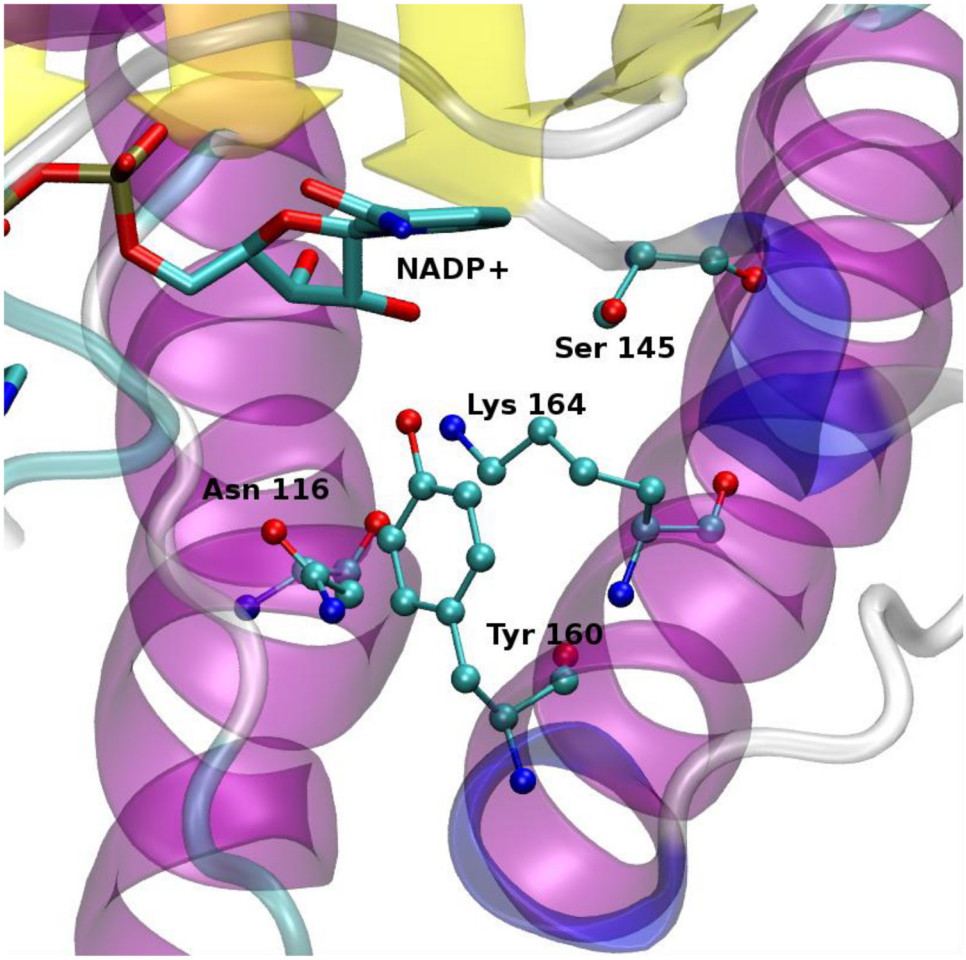

Figure 6. Model of the AaSDR1 active site with (E,E)-faruesol docked

Putative hydrogen bonds between (E,E)-farnesol and Tyr_{160} and Ser_{145} are shown in dotted lines. A putative interaction between the nicotinamide nng and (E,E)-farnesol is shown in dashed tines. $NADP^{+}$ and (E,E)-farnesol are drawn in balls and sticks representations whereas protein residues are shown in licorice. Carbon atoms are colored in cyan, nitrogen atoms are in blue and oxygen atoms are in red.

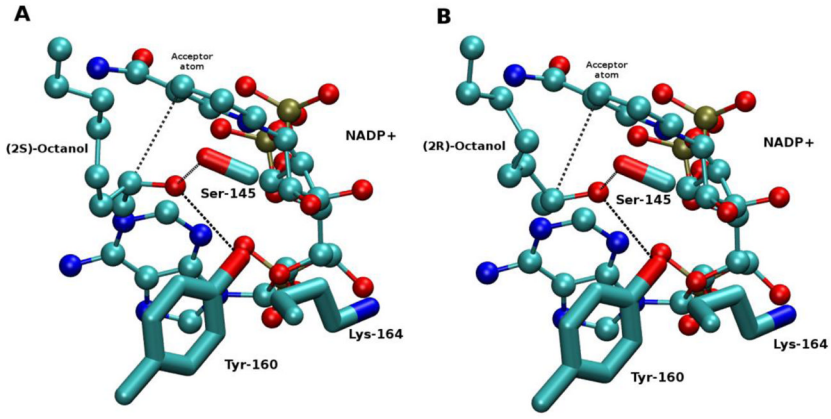

Figure 7. Dockiug of 2S- aud 2R-octauol

(A) 2S-octanol; (B) 2R-octanol. $NADP^+$ and (E,E)-farnesol are drawn in balls and sticks representations whereas protein residues are shown in licorice. Carbon atoms are colored in cyan, nitrogen atoms are in blue, oxygen atoms are in red and ochre color represents phosphorus atoms. Putative interaction between atoms are shown in dashed lines.

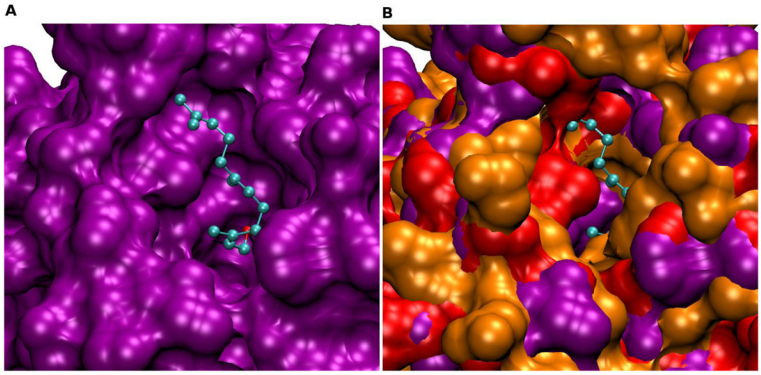

Figure 8. Active site surfaces of AaSDR1, AaSDR4 aud AaSDR9

(A) Active site of AaSDR1 (in violet) with (E,E)-farnesol docked. (B) Structural alignment of active sites of AaSDR4 (in red) and AaSDR9 (in orange) with (E,E)-farnesol docked.

Table 1

Expression of AaSDR RNAs at different life stages

PCR-based screening of the expression of AaSDR RNAs at different life stages.

	Larvae		Pupae		Adult ♀	CA
SDR	**3th**	**4th**	**0 h**	**24 h**	**3d**	**0–24h**
1	+	n.d.	n.d.	n.d.	+++	+++
2	+++	+++	+	+	+++	n.d.
3	n.d.	n.d.	n.d.	n.d.	+	n.d.
4	++	+	n.d.	n.d.	n.d.[1]	−
5	n.d.	n.d.	n.d.	n.d.	n.d.	−
7	+	+	+	n.d	++	n.d.
8	+	n.d.	+	+	++	n.d.
9	++	n.d.	+++	++	+++	n.d.

n.d.: not detected

+: relative amount

[1] Only detected in the accessory glands of the adult male.

Table 2A

substrate specificity

Substrate	SDR1	SDR2	SDR3	SDR4	SDR7	SDR8	SDR9
(E,E,E) Geranyl geraniol	6.1±0.1	nd	nd	nd	nd	nd	nd
(E,E) Farnesol	33.2±0.9	4.2±0.5	nd	nd	0.6±0.1	nd	1.1±0.2
(Z,Z) Farnesol	24.8±1.1	4.7±0.4	1.5±0.3	0.4±0.1	0.49±0.0	nd	2.7±0.3
Geraniol	55.1±1.7	0.6±0.1	0.2±0.1	nd	0.2±0.0	nd	0.4±0.0
Nerol	30.3±1.3	5.3±0.5	2.5±0.5	nd	0.4±0.0	nd	2.0±0.7
Citronellol	2.1±0.4	0.6±0.1	0.1±0.0	nd	0.5±0.0	nd	0.2±0.0
1-dodecanol	1.7±0.4	1.0±0.1	0.4±0.0	nd	0.7±0.1	Nd	0.5±0.0
2-dodecanol	57.7±1.3	42.1±0.9	0.9±0.2	6.0±0.5	5.2±0.1	1.0±0.3	37.4±2.0
2-decanol	67.1±0.3	30.9±0.1	1.6±0.1	12.0±0.6	3.4±0.3	3.2±0.5	34.6±1.9
1-Octanol	2.5±0.1	0.1±0.0	0.2±0.1	nd	0.6±0.1	nd	0.5±0.0
2-Octanol	43.5±0.3	13.8±1.6	2.1±0.2	6.7±0.9	2.3±0.8	0.3±0.4	27.4±2.3
1-Butanol	0.8±0.1	nd	0.2±0.0	nd	0.4±0.0	nd	nd
2-Butanol	3.7±0.2	nd	nd	nd	nd	nd	3.4±0.1
Ethanol	nd	nd	0.3±0.1	nd	0.7±0.2	nd	0.8±0.1
Glycerol	nd	nd	nd	nd	nd	nd	nd
Retinol	nd	nd	nd	nd	nd	nd	nd

Values are moles of substrate processed per mole of enzyme per min.

Table 2B

substrate stereo specificity

Substrate	SDR1	SDR2	SDR3	SDR4	SDR7	SDR8	SDR9
S-2-Octanol	156.2±1.7	28.8±0.5	2.8±0.9	7.6±1.4	2.8±0.0	nd	80.5±0.6
R-2-Octanol	9.1±0.8	2.9±0.1	1.3±0.3	0.9±0.1	3.2±0.0	nd	nd
S-2-Butanol	6.1±0.1	nd	nd	Nd	nd	nd	8.0±0.1
R-2-Butanol	1.1±0.1	nd	nd	nd	nd	nd	nd

Values are moles of substrate processed per mole of enzyme per min.

Table 3A

Effect of metal salts, inhibitors and reducing reagents (without pre-incubation).

Conc.	Compound	SDR1	SDR8
-	Control	100±0.1	100±0.2
0.05 mM	$ZnCl_2$	80.5±2.0	136.7±0.3
5 mM	$ZnCl_2$	78.3±0.4	96.1±10.8
10 mM	$ZnCl_2$	68.5±3.7	73.7±10.6
0.05 mM	$CuCl_2$	83.4±4.6	90.3±11.2
5 mM	$CuCl_2$	74.2±3.9	44.3±0.8
10 mM	$CuCl_2$	83.7±0.8	46.2±3.0
0.05 mM	$MgCl_2$	98.6±1.7	97.8±1.0
5 mM	$MgCl_2$	97.1±1.3	93.5±5.9
10mM	$MgCl_2$	100.9±0.37	82.3±8.6
3.5 mM	EDTA	86.8±1.0	86.9±3.2
0.05 mM	Iodoacetamide	87.3±0.6	87.0±1.6
5 mM	Iodoacetamide	86.6±0.8	-
10 mM	Iodoacetamide	87.3±0.6	-
0.01%	B-Mercaptoethanol	110.9±3.7	135.6±5.1
0.1%	B-Mercaptoethanol	132.1±14.6	131.1±4.7
1.0%	B-Mercaptoethanol	88.0±13.4	53.3±2.3
0.01%	DTT	101.7±3.0	163.1±4.1
0.1%	DTT	118.9±0.5	300.1±8.6
1.0%	DTT	82.1±2.4	367.5±26.2

Values are expressed as % of the control

Table 3B

Effect of metal salts, inhibitors and reducing reagents (with pre-incubation).

Conc.	Compound	SDR1	SDR8
-	Control	100±0.2	100±0.4
0.05 mM	$ZnCl_2$	93.9±6.0	8.5±3.3
5 mM	$ZnCl_2$	91.3±1.5	nd
10 mM	$ZnCl_2$	64.9±0.6	nd
0.05 mM	$CuCl_2$	nd	24.0±0.9
5 mM	$CuCl_2$	nd	nd
10 mM	$CuCl_2$	5.9±1.2	33.9±10.6
0.05 mM	$MgCl_2$	91±0.8	90±2.5
5 mM	$MgCl_2$	93.4±1.4	57.1±10.0
10mM	$MgCl_2$	97.3±1.3	21.4±2.6
3.5 mM	EDTA	68.9±2.2	63.8±6.6
0.05 mM	Iodoacetamide	53.7±6.0	79.4±5.6
5 mM	Iodoacetamide	72.4±14.5	-
10 mM	Iodoacetamide	62.3±19.4	-
0.01%	B-Mercaptoethanol	166.4±8.9	154.9±1.8
0.1%	B-Mercaptoethanol	279±8.9	149.6±1.4
1.0%	B-Mercaptoethanol	129.8±5.3	52.2±1.2
0.01%	DTT	103.6±6.9	252.8±24.0
0.1%	DTT	156.8±16.5	124.5±8.7
1.0%	DTT	138.2±12.1	nd

Values are expressed as % of the control